

## EXTREMAL DEPENDENCE ANALYSIS OF NETWORK SESSIONS

LUIS LÓPEZ-OLIVEROS AND SIDNEY I. RESNICK

ABSTRACT. We refine a stimulating study by Sarvotham et al. [2005] which highlighted the influence of peak transmission rate on network burstiness. From TCP packet headers, we amalgamate packets into sessions where each session is characterized by a 5-tuple  $(S, D, R, R^\vee, \Gamma)$ =(total payload, duration, average transmission rate, peak transmission rate, initiation time). After careful consideration, a new definition of peak rate is required. Unlike Sarvotham et al. [2005] who segmented sessions into two groups labelled alpha and beta, we segment into 10 sessions according to the empirical quantiles of the peak rate variable as a demonstration that the beta group is far from homogeneous. Our more refined segmentation reveals additional structure that is missed by segmentation into two groups. In each segment, we study the dependence structure of  $(S, D, R)$  and find that it varies across the groups. Furthermore, within each segment, session initiation times are well approximated by a Poisson process whereas this property does not hold for the data set taken as a whole. Therefore, we conclude that the peak rate level is important for understanding structure and for constructing accurate simulations of data in the wild. We outline a simple method of simulating network traffic based on our findings.

## 1. INTRODUCTION

Statistics on data networks show empirical features that are surprising by the standards of classical queuing theory. Two distinctive properties, which are called *invariants* in the network literature, are:

- Heavy tails for quantities such as file sizes [Arlitt and Williamson, 1996, Willinger and Paxson, 1998, Leland et al., 1994, Willinger et al., 1998], transmission durations and transmission delays [Maulik et al., 2002, Resnick, 2003].
- Network traffic is bursty [Sarvotham et al., 2005], with rare but influential periods of high transmission rate punctuating typical periods of modest activity. Burstiness is a somewhat vague concept but it is very important in order to understand network congestion.

When studying burstiness, bursts are observed in the sequence of bytes-per-time or packets-per-time, which means that a window resolution is selected and the number of bytes or packets is counted over consecutive windows. Sarvotham et al. [2005] attempt to explain the causes of burstiness at the user-level. By the user-level, we mean the clusters of bytes that have the same source and destination network addresses, which we term *sessions*. As a simplification, associate a session with a user downloading a file, streaming media, or accessing websites; a more precise definition is given later. For each session, measurements are taken on the size or number of bytes transmitted, the duration of the transmission and the average transfer rate. If the primary objective is to explain sources of burstiness, the session peak rate arises as a natural additional variable of interest. The peak rate is computed as the maximum transfer rate over consecutive time slots.

In order to explain the causes of burstiness at the user-level, Sarvotham et al. [2005] studied the dependence structure of quantities such as session size, duration and transfer rate. They concluded that it is useful to split the data into two groups according to the values of peak rate and consider the properties of each group. These two groups were called alpha sessions consisting of sessions whose peak rate is above a high quantile, and beta sessions, comprising the remaining traffic. Various criteria for segmenting into the two groups were considered but always the alpha group was thought of as sessions corresponding to “power

---

Luis López-Oliveros’ research was partially supported by CONACyT (Mexican Research Council of Science and Technology) Contract 161069. Sidney Resnick’s research was partially supported by ARO Contract W911NF-07-1-0078 at Cornell University.

users” who transmit large files at large bandwidth, and the beta group was the remaining sessions. This analysis yielded the following:

- A tiny alpha group relative to a huge beta group. In addition, it appeared that the alpha group was the major source of burstiness.
- A dependence structure that is quite different in the alpha and beta groups, with approximate independence between rate and size for the alpha group and approximate independence between rate and duration for the beta group. To see this, [Sarvotham et al. \[2005\]](#) measured dependence with correlations between the log-variables.

We wondered if the large beta group should be treated as one homogeneous collection of users, especially when one is happy to identify a small and distinct alpha group. Thus, we have investigated whether segmenting the beta group further produces meaningful information.

Section 2 contains more details on the network traffic traces that we study, and gives the precise definition of session, size, duration, rate and peak rate. Historically [[Crovella and Bestavros, 1997](#), [Leland et al., 1994](#), [Willinger et al., 1995, 1997](#)], data collection was over finely resolved time intervals, and thus a natural definition of peak rate is based on computing the maximum transfer rate over consecutive time slots. We discuss in Section 2 that this definition may be flawed due to the choice of the time window resolution giving the peak rate undesired properties. Thus we propose our own definition of peak rate.

In Section 3, we study the marginal distributions of size, duration and rate, and in Sections 4 and 5 we explore the dependence structure between these three variables. Throughout these sections, we depart from the approach of [Sarvotham et al. \[2005\]](#) by not just looking at the alpha and beta groups; instead, we have split the data into  $q$  groups of approximately equal size according to the quantiles of peak rate. Thus, where we previously had a beta group, we now have  $q - 1$  groups, whose peak rates are in a fixed quantile range. We show that the alpha/beta split is masking further structure and that it is important to take into account the explicit level of the peak rate. In Sections 4 and 5, we also review and use methods that are more suitable than correlation in the context of heavy tailed-modeling for studying the dependence of two variables.

We also have considered in Section 6 whether session starting times can be described by a Poisson process. While several authors have shown that the process of packet arrivals to servers cannot be modeled under the framework of Poisson processes [[Paxson and Floyd, 1995](#), [Willinger et al., 1997](#), [Willinger and Paxson, 1998](#), [Hohn et al., 2003](#)], some argue that the network traffic is driven by independent human activity and thus justify the search for this underlying Poisson structure at higher levels of aggregation [[Park et al., 2006](#)]. We have found that despite its inadequateness to describe the overall network traffic, a homogenous Poisson process is a good model for the session initiation times within each of the  $q$  groups produced by our segmentation of the overall traffic. In Section 7 we conclude with some final thoughts including a rough outline for simulation of data sets based on the aforementioned Poisson framework, and give possible lines of future study.

## 2. DEFINITIONS

**2.1. Size  $S$ , duration  $D$ , and rate  $R$  of e2e sessions.** Transmissions over a packet-switched computer network do not take place in a single piece, but rather in several small packets of data of bounded maximum size that depends on the specific network protocol. Thus, packet-level network traffic traces consist of records of packet headers, containing information of each individual packet such as arrival times to servers, number of bytes transmitted, source and destination network addresses, port numbers, network protocols, etc. As the packets travel across the network, routers and switches use the packet header information to move each packet to its correct destination. The two main goals of packet-switching are to optimize the utilization of available line bandwidth and to increase the robustness of communication [see e.g. [Keshav, 1997](#)].

The nature of the network data sets presents a challenge for modeling user behavior. Models such as a superimposition of on-off processes [[Willinger et al., 1997](#), [Sarvotham et al., 2005](#)] or an infinite-source Poisson model [[Guerin et al., 2003](#), [Maulik et al., 2002](#), [D’Auria and Resnick, 2006, 2008](#)] require a way to reconstruct from the individual packets either a suitable on-period for the former model, or a suitable transmission session, for the latter. One possible approach [[Sarvotham et al., 2005](#), [Willinger et al., 1997](#)]

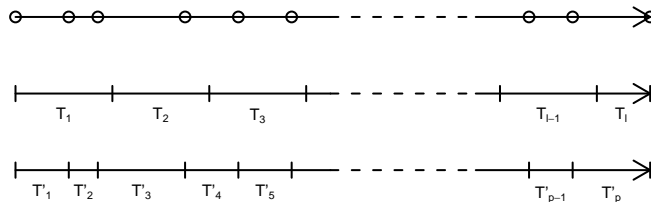


FIGURE 1. *Top arrow* Representation of a typical session; here each packet is depicted as an oval *Middle arrow* Sarvotham et al. [2005]’s division approach *Bottom arrow* Our proposed division according to the packet arrival times

is to define an *end to end (e2e) session*, or briefly session, as a cluster of bytes with the same source and destination network addresses, such that the delay between any two successive packets in the cluster is less than a threshold  $t$ . A session plays the role of an arriving entity in an infinite-source Poisson model or the role of an on-period in an on-off process model.

For each session, we have the following variables:

- $S$  represents the size, that is, the number of bytes transmitted.
- $D$  represents the duration, computed as the difference in seconds between the arrival times of the first and last packets in the session.
- $R$  represents the average transfer rate, namely  $S/D$ .

Note that  $R$  is not defined for single-packet sessions, for which  $D$  by definition is zero. More generally, sessions with very small  $D$  may also be problematic to handle. For instance, it would be hard to believe that a session sending only two packets back-to-back has an  $R$  that equals the line bandwidth. In order to avoid this issue, for our analysis we ignore sessions with  $D < 100ms$ . See Zhang et al. [2002] for related comments.

**2.2. Predictors of burstiness.** In addition to  $S$ ,  $D$  and  $R$ , Sarvotham et al. [2005] consider a fourth quantity which serves as an explanatory variable for burstiness, namely the session’s maximum input in consecutive time windows. A closely related variable arises by considering the session’s peak rate in consecutive intervals. In what follows, we review the properties of these two variables and show that they are not ideal for describing burstiness. Therefore, we will propose a different definition of peak rate.

**2.2.1. The  $\delta$ -maximum input.** Fix a small  $\delta > 0$  and divide each session in  $l$  subintervals of length  $\delta$ , where  $l = \lceil D/\delta \rceil$  (see Fig. 1, Top and Middle). For  $i = 1, \dots, l$ , define the following auxiliary variables:

- $B_i$  represents the number of bytes transmitted over the  $i$ th subinterval of the session.
- $T_i$  represents the duration of the  $i$ th subinterval. For  $i = 1, \dots, l - 1$ , we have  $T_i = \delta$ . However, notice that  $T_l = D - (l - 1)\delta$ .

The  $\delta$ -maximum input of the session is defined as  $I_\delta = \sqrt[n]{\prod_{i=1}^l B_i}$ . This  $I_\delta$  is the original variable used by Sarvotham et al. [2005].

**2.2.2. The  $\delta$ -peak rate.** If the goal is to explain burstiness, a natural alternative to maximum input is to consider rates in consecutive time subintervals, rather than inputs. This yields a closely related predictor: the  $\delta$ -peak rate. The definition of the  $\delta$ -peak rate for a session, denoted as  $R_\delta$ , relies on the Sarvotham et al. [2005]’s division of the session (see Fig. 1). We define  $R_\delta = \sqrt[n]{\prod_{i=1}^l B_i/T_i}$ .

Observe the following properties for a session:

- (i)  $\sum_{i=1}^n B_i = S$ ;
- (ii)  $\sum_{i=1}^n T_i = D$ ;
- (iii)  $R_\delta \geq R$ . To see this, note

$$R = \frac{S}{D} = \frac{\sum_{i=1}^n T_i \cdot \frac{B_i}{T_i}}{\sum_{i=1}^n T_i} \leq \bigvee_{i=1}^n B_i/T_i = R_\delta.$$

A quick analysis shows that the last property does not necessarily hold if we do not carefully define the duration of the last subinterval  $T_n$  as above, but instead set  $T_n = \delta$ . For a numerical example, let  $\delta = 1$  and consider a session with  $n = 2, B_1 = B_2 = 1, D = 1.1$ . Using the wrong definition  $T_n = \delta$  yields  $T_1 = T_2 = 1$ , hence the average transfer rate  $R = (B_1 + B_2)/D = 2/1.1$  but the peak transfer rate  $R_\delta = \max\{B_1/T_1, B_2/T_2\} = 1 < 2/(1.1)$ .

While both  $I_\delta$  and  $R_\delta$  appear to be natural predictors of burstiness, they both possess undesirable properties. They both depend on the parameter  $\delta$  which is not an intrinsic characteristic of the session. As  $\delta \downarrow 0$ , many consecutive subintervals thus have a single packet, as in Fig. 1. Therefore, as  $\delta \downarrow 0$ ,

- $I_\delta \rightarrow$  *maximum packet size*, which precludes  $I_\delta$  from being a useful measure of burstiness.
- $R_\delta \rightarrow \infty$ , implying that  $R_\delta$  is much greater than the line capacity as  $\delta \rightarrow 0$ . In fact, for this limit to hold, it is sufficient that a single subinterval has a few packets, which suggests that the convergence rate of  $R_\delta \rightarrow \infty$  is greater than the convergence rate of  $I_\delta \rightarrow$  *maximum packet size*. This implies that we still may have unreasonably large  $R_\delta$ s for relatively large  $\delta$ s. Therefore, the interpretation of  $R_\delta$  as an actual peak transfer rate becomes problematic.

Owing to the drawbacks of the previous two definitions, we propose our own definition of peak rate.

2.2.3. *Peak rate*  $R^\vee$ . Suppose a session has  $p$  packets (see Fig. 1, Bottom). Consider the following variables.

- $B'_i$  represents the number of bytes of the  $i$ th packet.
- $T'_i$  represents the interarrival time of the  $i$ th and  $(i + 1)$ th packets,  $i = 1, \dots, p - 1$ .

For  $k = 2, \dots, p$ , we define the *peak rate of order*  $k$ , denoted by  $R^{(k)}$ , as

$$R^{(k)} = \bigvee_{j=1}^{p-k+1} \frac{\sum_{i=j}^{j+k-1} B'_i}{\sum_{i=j}^{j+k-2} T'_i}. \quad (2.1)$$

In the above definition, the quotient measures the actual transfer rate of a stream of bytes consisting of  $k$  consecutive packets. For a session consisting of  $p$  packets, there are  $p - k + 1$  streams of  $k$  consecutive packets, hence  $R^{(k)}$  is a measure of the actual peak transfer rate when only  $k$  consecutive packets are taken into account. We then define the *peak rate* as

$$R^\vee = \bigvee_{k=2}^p R^{(k)}. \quad (2.2)$$

Notice that  $R^\vee \geq R^{(p)} = R$ .

As opposed to  $I_\delta$  and  $R_\delta$ ,  $R^\vee$  does not depend on external parameters such as  $\delta$ , and thus it is an intrinsic characteristic of a session. In addition,  $R^\vee$  inherits the interpretation of  $R^{(k)}$  and therefore it may be interpreted itself as a measure of the actual maximum transfer rate taken over all possible streams of consecutive packets. A drawback of our definition is that  $R^\vee$  is complex to analyze mathematically.

2.3. **The data set.** We present our results for a network trace captured at the University of Auckland between December 7 and 8, 1999, which was publicly available as of May 2009 through the National Laboratory for Applied Network Research website at <http://pma.nlanr.net/Special/index.html>. Auckland's data set is a collection of GPS-synchronized traces, where all non-IP traffic has been discarded and only TCP, UDP and ICMP traffic is present in the trace. We have taken the part of the trace corresponding exclusively to incoming TCP traffic sent on December 8, 1999, between 3 and 4 p.m. We have found that our results hold for several other data sets. See Section 7 for more details about this and other data traces.

The raw data consists of 1,177,497 packet headers, from which we construct 44,136 sessions using a threshold between sessions of  $t = 2s$  and considering only those sessions with  $D > 100ms$  (as explained in the last paragraph of Section 2.1). We have found similar results for various choices of thresholds between sessions, including  $t = 0.1, 0.5, 10, 60, 100s$ , but here we only present our results for  $t = 2s$ .

In addition, for each session we have peak rate  $R_i^\vee$  and starting time  $\Gamma_i$ . Thus, the data set has the form  $\{(S_i, D_i, R_i), R_i^\vee, \Gamma_i; 1 \leq i \leq 44,136\}$ , that is, a set of 5-tuples, but with the above notation we emphasize that the primary interest is placed on the dependence structure of triplet  $(S_i, D_i, R_i)$ .

We split these sessions into 10 groups of approximately equal size according to the empirical deciles of  $R^\vee$ . Thus, all the sessions in the  $g$ th group,  $g = 1, \dots, 10$ , have  $R^\vee$  in a fixed decile range,  $(10(g-1)\%, 10g\%]$ . Hence we term the group of sessions “the  $g$ th decile group”,  $g = 1, \dots, 10$ . Therefore, where Sarvotham et al. [2005] had alpha and beta groups, we now have a more refined segmentation.

In the remainder of the paper, we show that this refined split reveals features that are hidden by an elementary alpha/beta split.

### 3. MARGINAL DISTRIBUTIONS OF $S$ , $D$ AND $R$ .

In what follows, we analyze the marginal distributions of  $S$ ,  $D$  and  $R$  in the 10 different decile groups to check for the presence of one stylized fact in network data sets, namely, heavy tails. We found that  $S$  and  $D$  have heavy tails for all the different decile groups, but not  $R$ . Let us start by discussing background.

**3.1. Heavy tails and maximal domains of attraction.** A positive random variable  $Y$  has *heavy tails* if its distribution function  $F$  satisfies

$$1 - F(y) = \bar{F}(y) = y^{-1/\gamma}L(y), \quad (3.1)$$

where  $L$  is a slowly varying function and  $\gamma > 0$ . We also say that  $F$  is heavy tailed and we call  $\gamma$  the shape parameter. When  $F$  satisfies Eq. 3.1, it is also said to have regularly varying tails with tail index  $1/\gamma$ . Equation 3.1 is equivalent to the existence of a sequence  $b_n \rightarrow \infty$  such that

$$\mu_n(\cdot) := n\mathbb{P}\left[\frac{Y}{b_n} \in \cdot\right] \xrightarrow{v} c\nu_\gamma(\cdot), \quad (3.2)$$

vaguely in  $M_+(0, \infty]$ , the space of Radon measures on  $(0, \infty]$ . Here  $\nu_\gamma(x, \infty] = x^{-1/\gamma}$  and  $c > 0$ . Equation 3.2 is important for generalizing the concept of heavy tailed distributions to higher dimensions.

An important concept is maximal domains of attraction. Suppose  $\{Y_i; i \geq 1\}$  is iid with common distribution  $F$ . The distribution  $F$  is in the *maximal domain of attraction* of the extreme value distribution  $G_\gamma$ , denoted  $F \in \mathcal{D}(G_\gamma)$ , if there exist sequences  $a_n > 0$  and  $b_n \in \mathbb{R}$  such that for  $y \in \mathbb{E}^{(\gamma)} = \{y \in \mathbb{R} : 1 + \gamma y > 0\}$ :

$$\lim_{n \rightarrow \infty} \mathbb{P}\left[\frac{\bigvee_{i=1}^n Y_i - b_n}{a_n} \leq y\right] = G_\gamma(y) := \exp\{-(1 + \gamma y)^{-1/\gamma}\}. \quad (3.3)$$

This is equivalent to the existence of functions  $a(t) > 0$  and  $b(t) \in \mathbb{R}$  such that for  $y \in \mathbb{E}^{(\gamma)}$ :

$$\lim_{t \rightarrow \infty} t\mathbb{P}[Y_1 > a(t)y + b(t)] = -\log G_\gamma(y). \quad (3.4)$$

The class of distributions  $\mathcal{D}(G_\gamma)$  is known as the Fréchet domain when  $\gamma > 0$ , Gumbel domain when  $\gamma = 0$  and Weibull domain when  $\gamma < 0$ . Equation 3.3 is also known as the extreme value condition.

For  $\gamma > 0$ ,

$$\bar{F}(y) = y^{-1/\gamma}L(y) \Leftrightarrow F \in \mathcal{D}(G_\gamma), \quad (3.5)$$

for some slowly varying  $L$ . In other words, a necessary and sufficient condition for a distribution to be heavy tailed is that it is in the Fréchet class [de Haan and Ferreira, 2006, Resnick, 1987].

Thus, the focus will be placed on checking the Fréchet domain condition. First, we check whether or not the marginals of  $(S, D, R)$  are in some domain of attraction. If that turns out to be the case, we proceed to check for the specific domain class.

### 3.2. Domain of attraction diagnostics.

3.2.1. *Excesses over high thresholds.* One common method [Davison and Smith, 1990, Beirlant et al., 2004, Coles, 2001, Reiss and Thomas, 2007, McNeil et al., 2005, de Haan and Ferreira, 2006] to check the extreme value condition, given by Eq. 3.3, relies on threshold excesses, using all data that are “extreme” in the sense that they exceed a particular designated high level.

More precisely, consider a random variable  $Y$  with distribution function  $F$ . Given realizations of  $Y$ , say  $y_1, \dots, y_n$  and a threshold  $u$ , we call  $y_j$  an exceedance over  $u$  if  $y_j > u$ , and in such case,  $y_j - u$  is called the *excess*. Denote the *excess distribution* over the threshold  $u$  as  $F_u$ , i.e.

$$F_u(y) = \mathbb{P}[Y - u \leq y | Y > u],$$

for all  $0 \leq y \leq y_F - u$ , where  $y_F \leq \infty$  is the right endpoint of  $F$ . The connection with domains of attraction is that

$$F \in \mathcal{D}(G_\gamma) \Leftrightarrow \lim_{u \rightarrow y_F} \sup_{0 \leq y \leq y_F - u} |F_u(y) - GPD_{\gamma, \beta(u)}(y)| = 0, \text{ for some } \beta(u) > 0. \quad (3.6)$$

Here  $GPD_{\gamma, \beta}$ , with  $\gamma \in \mathbb{R}, \beta > 0$  is the generalized Pareto distribution, defined as

$$GPD_{\gamma, \beta}(y) := 1 - (1 + \gamma y / \beta)^{-1/\gamma},$$

for  $y \geq 0$  when  $\gamma \geq 0$  and  $0 \leq y \leq -\beta/\gamma$  when  $\gamma < 0$ . See Pickands [1975], Balkema and de Haan [1974], de Haan and Ferreira [2006].

For a distribution  $F$ , the method of excesses over high thresholds (also referred to as peaks over thresholds or *POT*) assumes equality in Eq. 3.6 holds for a high threshold  $u$ , without need to take a limit, meaning that the excess distribution over such  $u$  equals a generalized Pareto distribution. See Embrechts et al. [1997], Coles [2001], Reiss and Thomas [2007], de Haan and Ferreira [2006]. Thus, suppose  $Y_1, \dots, Y_n$  are iid with common distribution  $F$  and let  $Y_{1:n} \leq Y_{2:n} \leq \dots \leq Y_{n:n}$  be the order statistics. Fix a high threshold  $\hat{u} = Y_{n-k:n}$  as the  $(k+1)$ th largest statistic, and fit a  $GPD_{\gamma, \beta}$  model to  $Y_{n-k+1:n} - \hat{u}, \dots, Y_{n:n} - \hat{u}$ . Then the evidence supports  $F \in \mathcal{D}(G_\gamma)$  if and only if for some high threshold  $\hat{u}$  that fit is adequate. For informally assessing the goodness of fit, we compare via quantile-quantile (QQ) plots the sample quantiles, namely  $\hat{Y}_{n-k+1:n} - \hat{u}, \dots, \hat{Y}_{n:n} - \hat{u}$ , against the theoretical quantiles given by the  $GPD$  fit. It is not difficult to show that  $Z \sim GPD_{\gamma, \beta}$  is equivalent to the statement that  $\log(1 + \gamma Z / \beta) / \gamma \sim \exp(1)$ , and so we draw QQ plots in this latter scale after estimating  $\gamma, \beta$  by means of, say, maximum likelihood.

Using the POT method, we found no evidence against  $F_S, F_D \in \mathcal{D}(G_\gamma)$  for all the 10 decile groups. Typical QQ plots are those corresponding to the  $GPD_{\gamma, \beta}$  fit for the excess of  $S$  and  $D$  in the 10th decile group, shown in Fig. 2, *Upper left* and *Upper right* panels, respectively. Both plots exhibit an almost perfect straight line. We also found that the QQ plots corresponding to the excesses of  $S$  and  $D$  in all the other decile groups exhibit straight line trends, showing thus no evidence against satisfaction of the extreme value condition.

Similarly, Fig. 2 *Lower left* panel exhibits the QQ plot of the  $GPD_{\gamma, \beta}$  fit for the excess of  $R$  in the 10th decile group, which shows no evidence against  $F_R \in \mathcal{D}(G_\gamma)$ . However, for all the other decile groups, we found evidence against  $F_R \in \mathcal{D}(G_\gamma)$ . For instance, a QQ plot of the  $GPD_{\gamma, \beta}$  fit for the excess of  $R$  in the 4th decile group is shown in Fig. 2 *Lower right* panel, exhibiting a major departure from the straight line. We also found no straight line trend in the rest of the QQ plots of the  $GPD_{\gamma, \beta}$  fit for the excess of  $R$  in the lower nine decile groups.

3.2.2. *Formal tests of domain of attraction.* Recently, two formal methods for testing  $F \in \mathcal{D}(G_\gamma)$  have been derived by Dietrich et al. [2002] and Drees et al. [2006]. Both tests are similar in that the two are based on quantile function versions of the well known Crámer von-Mises and Anderson-Darling test statistics [see e.g. Lehmann and Romano, 2005], respectively, for checking the goodness of fit of a given distribution. In addition, both tests assume a so called second order condition which is difficult to check in practice. A follow-up study by Hüsler and Li [2006] examines the two tests’ error and power by simulations. A thorough discussion of these tests and the second order condition is provided by de Haan and Ferreira [2006]. Here we review the method proposed in Dietrich et al. [2002] and use it to test for the extreme value condition.



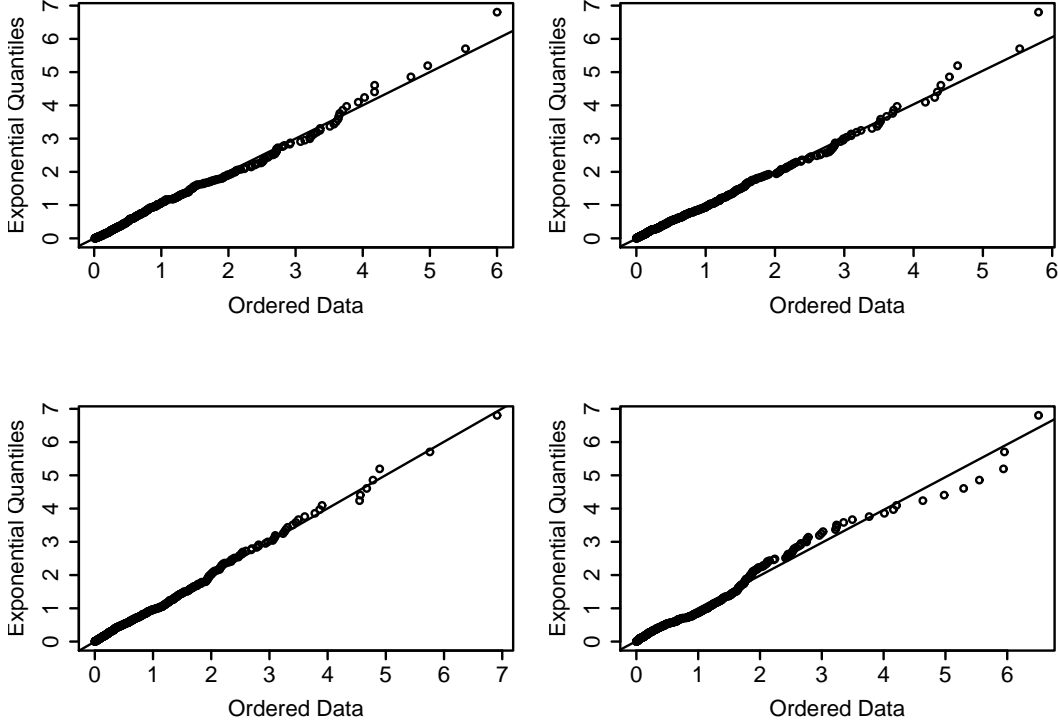


FIGURE 2. *GPD* QQ-plots of excesses; a number  $k = 450$  of upper order statistics is used for each fit *Upper left* Size in the 10th decile group *Upper right* Duration in the 10th decile group *Lower left* Rate in the 10th decile group *Lower right* Rate in the 4th decile group

Dietrich et al. [2002] state that if  $F \in \mathcal{D}(G_\gamma)$  for some  $\gamma \in \mathbb{R}$  and also if  $F$  satisfies an additional second order tail condition [for the details of this condition, see Dietrich et al., 2002, equation (4)], then:

$$\begin{aligned}
 E_{k,n} &:= k \int_0^1 \left( \frac{\log Y_{n-[kt]:n} - \log Y_{n-k:n}}{\hat{\gamma}_+} - \frac{t^{-\hat{\gamma}_-} - 1}{\hat{\gamma}_-} \right) t^2 dt \\
 \xrightarrow{d} E_\gamma &:= \int_0^1 \left( (1 - \gamma_-)(t^{-\gamma_- - 1} W(t) - W(1)) - (1 - \gamma_-)^2 \frac{t^{-\gamma_-} - 1}{\gamma_-} P_{\gamma_-} \right. \\
 &\quad \left. + \frac{t^{-\gamma_-} - 1}{\gamma_-} R_{\gamma_-} + (1 - \gamma_-) R_{\gamma_-} \int_t^1 s^{-\gamma_- - 1} \log s ds \right)^2 t^2 dt, \tag{3.7}
 \end{aligned}$$

as  $k \rightarrow \infty, k/n \rightarrow 0, n \rightarrow \infty$  and  $k^{1/2} A(n/k) \rightarrow 0$ , where  $A$  is related to the second order condition,  $\gamma_+ = \max\{\gamma, 0\}$  and  $\gamma_- = \min\{\gamma, 0\}$ ,  $W$  is a Brownian motion,  $P_{\gamma_-}$  and  $R_{\gamma_-}$  are some integrals involving  $W$  [for the details, see Dietrich et al., 2002, de Haan and Ferreira, 2006], and  $\hat{\gamma}_+$  and  $\hat{\gamma}_-$  are consistent estimators of the corresponding parameters.

In practice, Dietrich et al. [2002] recommend replacing  $\gamma$  by its estimate. Therefore, based on Eq. 3.7, we could test

$$H_0 : F \in \mathcal{D}(G_\gamma), \gamma \in \mathbb{R} + \text{second order condition}$$

by first determining the corresponding quantile  $Q_{1-\alpha, \hat{\gamma}}$  of the distribution  $E_{\hat{\gamma}}$  and then comparing it with the value of  $E_{k,n}$ . If  $E_{k,n} > Q_{1-\alpha, \hat{\gamma}}$  we reject  $H_0$  with asymptotic type I error  $\alpha$  and otherwise there is no evidence to reject  $H_0$ . Notice that this is a one-sided test of hypothesis, but a two-sided test could be performed in a similar fashion.

A drawback of this test is that we must include in  $H_0$  the additional second order condition, which is difficult to check in practice. While many common distributions satisfy the second order condition, including the normal, stable, Cauchy, log-Gamma, among others, the Pareto distribution is a notable example of a distribution which does not satisfy the second order condition.

In addition, there are two other drawbacks of this test. First, it is based on the usual setting of acceptance-rejection regions, and thus it provides no measure of the strength of rejection of  $H_0$ . While this typically is addressed with the equivalent setting based on p-values, the limit distribution in Eq. 3.7 is analytically intractable and so are the p-values. Second, since the limit in Eq. 3.7 depends on  $k$ , the conclusions of the test are also highly dependent on the choice of  $k$ .

Dietrich et al. [2002] state a corollary in which the limit distribution in Eq. 3.7 is greatly simplified by observing that  $\gamma_- = 0$  for all  $\gamma \geq 0$ . This result is easier to apply. Under the assumption that  $F \in \mathcal{D}(G_\gamma)$ ,  $\gamma \geq 0$  and the second order condition, Eq. 3.7 becomes:

$$\begin{aligned} \tilde{E}_{k,n} &= k \int_0^1 \left( \frac{\log Y_{n-[kt]:n} - \log Y_{n-k:n}}{\hat{\gamma}_{k,n}} + \log t \right)^2 t^2 dt \\ \xrightarrow{d} \tilde{E} &= \int_0^1 \left( t^{-1} W_t - W_1 + \log t \int_0^1 (s^{-1} W_s - W_1) ds \right)^2 t^2 dt. \end{aligned} \quad (3.8)$$

Suppose  $\tilde{E}_1, \dots, \tilde{E}_N$  is a random sample of  $\tilde{E}$ , that we can obtain by simulation since the limit distribution in Eq. 3.8 is free of unknown parameters. Based on Eq. 3.8, we propose the following test for

$$H_0 : F \in \mathcal{D}(G_\gamma), \gamma \geq 0 + \text{second order condition.}$$

Estimate a (one-sided) p-value  $p(k) = \mathbb{P}(\tilde{E} > \tilde{E}_{k,n})$  as the relative frequency

$$\hat{p}(k) = \frac{1}{N} \sum_{j=1}^N 1_{\tilde{E}_j > \tilde{E}_{k,n}}.$$

If  $\hat{p}(k) < \alpha$ , then reject  $H_0$  with an asymptotic type I error  $\alpha$ , otherwise there is no evidence to reject  $H_0$ . With this method, the p-values give a measure of the strength of rejection of  $H_0$ . Furthermore, we can check the stability of the conclusion of the test as a function of  $k$  by constructing the plot  $\{(k, \hat{p}(k)); k \text{ in an appropriate range}\}$ . The range of values of  $k$  is chosen to accommodate for the limit in Eq. 3.8, namely  $k \rightarrow \infty, k/n \rightarrow 0, n \rightarrow \infty$ . For example, Hüsler and Li [2006] found via simulations that the power of the test in Dietrich et al. [2002] appears to be high for  $k$  such that  $k/n \approx 0.05$ , at least for their various choices of  $F$ . To compute  $\tilde{E}_{k,n}$ , we use  $\hat{\gamma}_{k,n}$  given by the consistent Hill estimator [Hill, 1975] or perhaps maximum likelihood if we suspect  $\gamma = 0$ .

We use this method with an asymptotic nominal type I error  $\alpha = 0.05$ . We found no evidence against  $F_S, F_D \in \mathcal{D}(G_\gamma), \gamma \geq 0$  for all the 10 decile groups. Typical plots of the p-values  $\hat{p}(k)$  for the variables  $S$  and  $D$  are those corresponding to the 10th decile group, shown in Fig. 3 Upper left and Upper right panels, respectively. Both plots exhibit that  $\hat{p}(k) > 0.05$  for a wide range of values of  $k$ . We also found here that the plots  $\{(k, \hat{p}(k))\}$  corresponding to all the other decile groups show no evidence against  $F_S, F_D \in \mathcal{D}(G_\gamma), \gamma \geq 0$ . Coupled with the evidence from the QQ plots, we believe  $\gamma > 0$ .

Similarly, Fig. 3 Lower left exhibits the plot  $\{(k, \hat{p}(k))\}$  corresponding to the distribution of  $R$  in the 10th decile group. Once again we found that  $\hat{p}(k) > \alpha$  for a wide range of values of  $k$ , thus showing no evidence against  $F_R \in \mathcal{D}(G_\gamma), \gamma \geq 0$ . However, we did find evidence against  $H_0 : F_R \in \mathcal{D}(G_\gamma), \gamma \geq 0 + \text{second order condition}$  for all the lower nine decile groups. A typical example of the plot  $\{(k, \hat{p}(k))\}$  in these latter groups is exhibited in Fig. 3 Lower right for the 4th decile group, which shows that  $\hat{p}(k)$  are significantly lower than 0.05 across a wide range of  $k$  values.

Therefore, for the lowest nine decile groups, we reject  $H_0 : F_R \in \mathcal{D}(G_\gamma), \gamma \geq 0 + \text{second order condition}$ . One possible alternative is that  $F_R \in \mathcal{D}(G_\gamma), \gamma < 0$ , or equivalently, that  $x_{F_R} < \infty$  and  $F_{(x_{F_R} - R)^{-1}} \in \mathcal{D}(G_{-1/\gamma})$  [de Haan and Ferreira, 2006, Resnick, 1987]. Hence, by applying the above test to  $H_0 : F_{(x_{F_R} - R)^{-1}} \in \mathcal{D}(G_\gamma), \gamma \geq 0 + \text{second order condition}$ , we dropped the possibility of this new  $H_0$  because the  $\hat{p}(k) < 0.05$  for



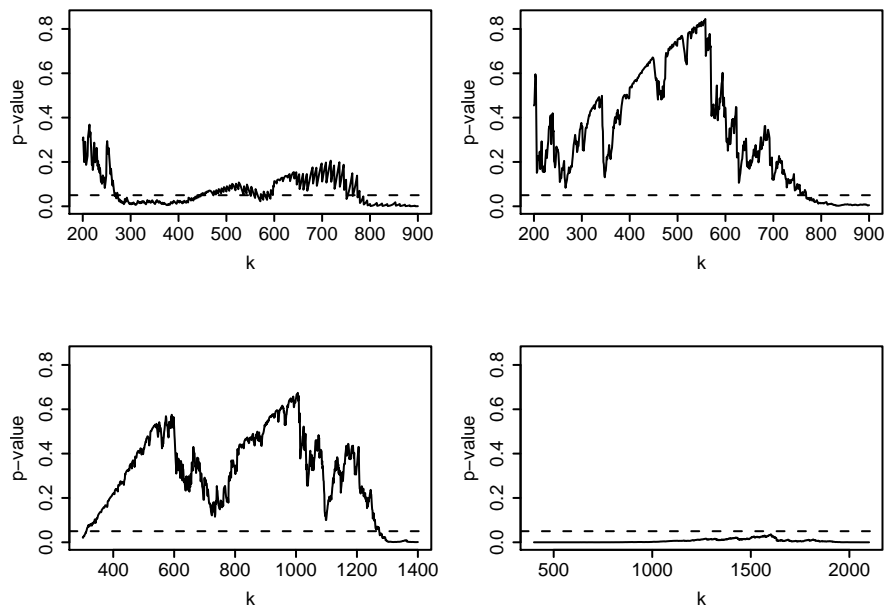


FIGURE 3. Plots of p-values as a function of  $k$  for the test of the extreme value condition for the distribution of the following variables; a horizontal dashed line is drawn at  $\alpha = 0.05$  *Upper left* Size in the 10th decile group *Upper right* Duration in the 10th decile group *Lower left* Rate in the 10th decile group *Lower right* Rate in the 4th decile group

a wide range of values of  $k$  for the lower nine decile groups. Here we estimated  $x_{F_R}$  with  $R_{n:n} + 1/n'$  for a high value of  $n'$ .

This last result left us with two possibilities. Either  $F_R \notin \mathcal{D}(G_\gamma), \gamma \in \mathbb{R}$  or simply, the additional second order condition does not apply for  $F_R$  (and in this case we still may have  $F_R \in \mathcal{D}(G_\gamma), \gamma \geq 0$ ). As previously mentioned, the second order condition is difficult to check in practice without any prior knowledge of the distribution function, and thus the hypothesis test fails to provide a clear description of the distribution  $F_R$ . Nevertheless, in Section 5 we are able to say something about  $F_R$ .

**3.3. Estimation.** In Section 3.2.2 we showed that  $F_S, F_D \in \mathcal{D}(G_\gamma), \gamma \geq 0$  for all the decile groups and  $F_R \in \mathcal{D}(G_\gamma), \gamma \geq 0$  only for the 10th decile group. We now proceed to the estimation of the shape parameter  $\gamma$  for these distributions.

The Hill estimator is a popular estimator of  $\gamma$  [Hill, 1975, Csörgő et al., 1985, Davis and Resnick, 1984, de Haan and Resnick, 1998, Hall, 1982]. The *Hill estimator* based on the  $k$  largest order statistics is

$$\hat{\gamma}_{k,n} = \frac{1}{k} \sum_{i=n-k+1}^n \log \frac{Y_{i:n}}{Y_{n-k:n}}, \quad k = 1, \dots, n-1. \quad (3.9)$$

For  $F \in \mathcal{D}(G_\gamma), \gamma > 0$ , the Hill estimator  $\hat{\gamma}_{k,n}$  is a consistent estimator of  $\gamma$ . Furthermore, under an additional second order condition of the type needed in Eq. 3.7:

$$\sqrt{k}(\hat{\gamma}_{k,n} - \gamma) \xrightarrow{d} N(0, \gamma^2), \quad (3.10)$$

so both consistency and asymptotic normality hold as  $k \rightarrow \infty, k/n \rightarrow 0$ , and  $n \rightarrow \infty$ . See, for example, de Haan and Ferreira [2006], Resnick [2007], Geluk et al. [1997], de Haan and Resnick [1998], Peng [1998], de Haan and Peng [1998], Mason and Turova [1994].

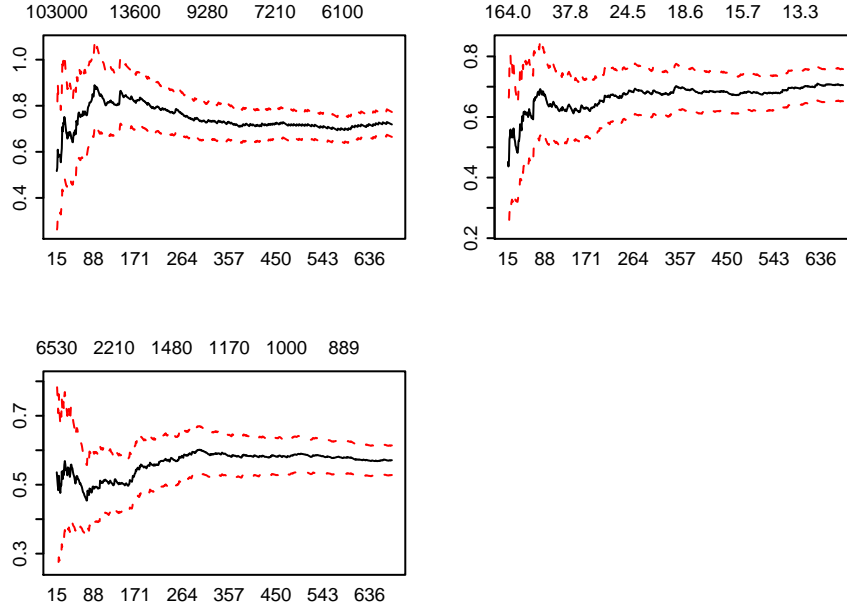


FIGURE 4. Hill plots, with 95% confidence bands in dashed lines, corresponding to the shape parameter  $\gamma$  of the variables in the 10th decile group; the values on top give thresholds and the values on bottom indicate the number of upper order statistics *Upper left Size Upper right Duration Lower left Rate*

The Hill estimator depends on the number  $k$  of upper-order statistics and so in practice, we make a *Hill plot*  $\{(k, \hat{\gamma}_{k,n}); k \geq 1\}$  and pick a value of  $\hat{\gamma}_{k,n}$  for which the graph looks stable. Figure 4 exhibits Hill plots for the shape parameter  $\gamma$  of the distribution of  $S$ ,  $D$  and  $R$  for the 10th decile group. The three plots show stable regimes for  $\gamma$  around  $k = 450$ . We also found stability in the Hill plots for the shape parameter  $\gamma$  of the distribution of  $S$ ,  $D$  in all the other decile groups.

Table 1 contains the Hill estimates of  $\gamma$  for our data set, along with estimates of the asymptotic standard error based on Eq. 3.10. A number  $k$  of upper order statistics was chosen individually for each variable and each decile group based on the corresponding Hill plots. For most decile groups, we used  $k \approx 400$  ( $k/n \approx 0.05$ ), as suggested by the empirical study by Hüsler and Li [2006]. Notice that the majority of the estimates are greater than 0.5, which implies that the corresponding distributions have infinite variances.

We make some final comments on our choice of the Hill estimator against the Pickands estimator [Pickands, 1975, Dekkers and de Haan, 1989]. In Section 3.2.2 we only showed that  $\gamma \geq 0$  which is a weaker assumption than the requirement of  $\gamma > 0$  for the Hill estimator. Unlike the Hill estimator, the Pickands estimator is more robust in the sense that it does not need  $\gamma > 0$ . However, the *Pickands plots* proved to be very unstable for our data set.

#### 4. DEPENDENCE STRUCTURE OF $(S, D, R)$ WHEN THE THREE VARIABLES HAVE HEAVY TAILS

We now analyze the dependence structure of the triplet  $(S, D, R)$  across the 10 different decile groups. Since  $S = DR$ , at most two of the three components in  $(S, D, R)$  may be independent. This makes it reasonable to focus on the analysis of each pair of variables. We concentrate on the pairs in  $(S, D, R)$  with heavy tailed marginals and first focus on the dependence structure of  $(S, D)$  across the 10 deciles groups. We later study the dependence structure of both  $(R, S)$  and  $(R, D)$ , but only in the 10th decile group. For the other decile groups, we found strong evidence suggesting  $R$  does not have heavy tails, and thus we leave this

TABLE 1. Summary of Hill estimates with asymptotic standard errors for the shape parameter of  $S$ ,  $D$  and  $R$ 

Decile group	$\gamma_S$	s.e.	$\gamma_D$	s.e.	$\gamma_R$	s.e.
1	0.56	0.056	0.60	0.028		
2	0.55	0.061	0.47	0.023		
3	0.62	0.044	0.63	0.034		
4	0.62	0.036	0.62	0.029		
5	0.61	0.035	0.55	0.029		
6	0.69	0.040	0.55	0.028		
7	0.88	0.042	0.73	0.037		
8	0.77	0.045	0.71	0.033		
9	0.70	0.037	0.69	0.032		
10	0.73	0.034	0.68	0.032	0.58	0.027

case for Section 5. Our finer segmentation into the deciles of  $R^\vee$  reveals hidden features in an alpha/beta split, and therefore it is important to take into account the explicit level of  $R^\vee$ .

One way to assess the dependence structure is with sample cross-correlations. In heavy-tailed modeling, although the sample correlations may always be computed, there is no guarantee that the theoretical correlations exist. Recall Table 1 shows that most estimates of  $\gamma$  for  $S$ ,  $D$  and  $R$  are greater than 0.5, and thus correlations do not exist in these instances. Moreover, correlation is a crude summary of dependence that is most informative between jointly normal variables, and that certainly does not distinguish between the dependence between large values and the dependence between small values. In the context of data networks, the likelihood of various simultaneous large values of  $(S, D, R)$  may be important for understanding burstiness. For example, if large values of  $D$  are likely to occur simultaneously with large values of  $R$ , then we can expect a network that is prone to congestion. In this situation, a scatterplot  $\{(D_i, R_i)\}$  would be mostly concentrated in the interior of the first quadrant of  $\mathbb{R}^2$ . On the other hand, if large values of one variable are not likely to occur with large values of the other one, the same scatterplot would be mostly concentrated on the axes.

Understanding network behavior requires a description of the extremal dependence of  $S, D$  and  $R$  and this extremal dependence is conveniently summarized by the spectral measure. See [de Haan and Resnick \[1977\]](#), [de Haan and Ferreira \[2006\]](#), [Resnick \[2007, 2008\]](#). We begin by discussing important concepts.

**4.1. Bivariate regular variation and the spectral measure.** Let  $\mathbf{Z}$  be a random vector on  $\mathbb{E} := [0, \infty]^2 \setminus \{(0, 0)\}$ , with distribution function  $F$ . The tail of  $F$  is *bivariate regularly varying* if there exist a function  $b(t) \rightarrow \infty$  and a Radon measure  $\nu$  on  $\mathbb{E}$ , such that

$$t\mathbb{P}\left[\frac{\mathbf{Z}}{b(t)} \in \cdot\right] \xrightarrow{v} \nu(\cdot), \quad (4.1)$$

vaguely in  $\mathbb{E}$ . Notice that this is a straightforward generalization of the univariate case as formulated in Eq. 3.2.

In terms of dependence structure of the components of  $\mathbf{Z}$ , it is often illuminating to consider the equivalent formulation of Eq. 4.1 that arises by transforming to polar coordinates. We define the *polar coordinate* transform of  $\mathbf{Z} = (X, Y) \in \mathbb{E}$  by

$$(N, \Theta) = \text{POLAR}(\mathbf{Z}) := \left( \|\mathbf{Z}\|, \frac{\mathbf{Z}}{\|\mathbf{Z}\|} \right), \quad (4.2)$$

where from this point on we use the  $L_1$  norm given by  $\|\mathbf{Z}\| = X + Y$ .

Bivariate regular variation as formulated in Eq. 4.1 is equivalent to the existence of a function  $b(t) \rightarrow \infty$  and a probability measure  $\mathbb{S}$  on  $\mathfrak{N}_+$ , where  $\mathfrak{N}_+ = \{\mathbf{z} \in \mathbb{E}; \|\mathbf{z}\| = 1\}$ , such that

$$\mu_t(\cdot) := t\mathbb{P}\left[\left(\frac{N}{b(t)}, \Theta\right) \in \cdot\right] \xrightarrow{v} c\nu_\gamma \times \mathbb{S}(\cdot), \quad (4.3)$$

vaguely in  $M_+((0, \infty] \times \mathfrak{N}_+)$ . Here  $\nu_\gamma(r, \infty] = r^{-1/\gamma}$ ,  $r > 0$ , and  $c > 0$  and, as usual,  $M_+((0, \infty] \times \mathfrak{N}_+)$  are the positive Radon measures on  $(0, \infty] \times \mathfrak{N}_+$ . Since there is a natural bijection between  $\mathfrak{N}_+$  and  $[0, 1]$ , namely  $\frac{\mathbf{z}}{\|\mathbf{z}\|} \leftrightarrow \frac{X}{\|Z\|}$ , we can and will assume  $\mathbb{S}$  is defined on  $[0, 1]$ .

The probability measure  $\mathbb{S}$  is known as the *limit* or *spectral measure*, and it quantifies the dependence structure among the components of the bivariate random vector. Consider the following two cases which represent opposite ends of the dependence spectrum [Coles, 2001, Resnick, 2007]. Suppose  $\mathbf{Z} = (X, Y)$  is a random vector in  $\mathbb{E}$  that is bivariate regularly varying as in Eq. 4.3.

- On one end of the dependence spectrum, if  $\mathbf{Z} = (X, Y)$  and  $X$  and  $Y$  are iid, then  $\mathbb{S}$  concentrates on  $\theta \in \{0, 1\}$ , corresponding to the axis  $x = 0$  and  $y = 0$ , respectively. Conversely, if  $\mathbb{S}$  concentrates on  $\theta \in \{0, 1\}$ , then there is negligible probability that both  $X$  and  $Y$  are simultaneously large, and this behavior is called *asymptotic independence*.
- On the other end of the dependence spectrum, if  $\mathbf{Z} = (X, Y)$  and  $X = Y$ , the two components are fully dependent and  $\mathbb{S}$  concentrates on  $\theta = 1/2$ . This behavior is called *asymptotic full dependence*. If  $\mathbb{S}$  concentrates on the interior of the  $\mathbb{E}$ , then we can expect  $X$  and  $Y$  to be highly dependent.

Since  $\mathbb{S}$  could be any probability measure, there are infinitely many kinds of dependence structures between the two extreme cases discussed above. Therefore, we focus on the estimation of the spectral measure  $\mathbb{S}$  as means of discerning the asymptotic dependence between two random variables with heavy tails.

**4.2. Estimation of the spectral measure  $\mathbb{S}$  by the antiranks method.** For estimating  $\mathbb{S}$ , we use the following result. If  $\{\mathbf{Z}_i, i = 1, \dots, n\}$  is a random sample of iid vectors in  $\mathbb{E}$  whose common distribution  $F$  is bivariate regularly varying as in Eq. 4.1, then for  $(N_i, \Theta_i) := \left(\|\mathbf{Z}_i\|, \frac{\mathbf{Z}_i}{\|\mathbf{Z}_i\|}\right)$ :

$$\frac{1}{k} \sum_{i=1}^n \epsilon_{(N_i/b(\frac{n}{k}), \Theta_i)} \Rightarrow c\nu_\gamma \times \mathbb{S}, \quad (4.4)$$

as  $k \rightarrow \infty, k/n \rightarrow 0$ , and  $n \rightarrow \infty$ . Equation 4.4 provides a consistent estimator of  $\mathbb{S}$ , since

$$\frac{\sum_{i=1}^n \epsilon_{(N_i/b(\frac{n}{k}), \Theta_i)}((1, \infty] \times \cdot)}{\sum_{i=1}^n \epsilon_{N_i/b(\frac{n}{k})}((1, \infty])} \Rightarrow \mathbb{S}(\cdot), \quad (4.5)$$

provided  $b(t) = t$ . See Huang [1992], de Haan and Ferreira [2006], Resnick [2007].

However, the phrasing of bivariate regular variation in Eq. 4.1 requires scaling the two components of  $\mathbf{Z} = (X, Y)$  by the same factor, which implies that

$$n\mathbb{P}\left[\frac{X}{b_n} \in \cdot\right] \xrightarrow{v} c_1\nu_\gamma(\cdot), \quad n\mathbb{P}\left[\frac{Y}{b_n} \in \cdot\right] \xrightarrow{v} c_2\nu_\gamma(\cdot), \quad n \rightarrow \infty$$

for  $c_j \geq 0$  and  $j = 1, 2$ . When  $c_1 > 0$  and  $c_2 > 0$ , both  $X$  and  $Y$  have the same shape parameters and their distributions are tail equivalent [Resnick, 1971]; this is the *standard regular variation* case.

In practice, we rarely encounter bivariate heavy tailed data for which the  $\gamma$  of each component is the same. For example, consider the bivariate random vector  $(S, D)$ . For many decile groups, observe in Table 1 that  $\gamma_S \neq \gamma_D$ . Hence, in order to estimate  $\mathbb{S}$ , one possible approach is to transform the data to the standard case using the antiranks method [Huang, 1992, de Haan and Ferreira, 2006, Resnick, 2007]. This procedure does not require estimation of the  $\gamma$ s, yet it achieves transformation to the standard case, thus allowing the estimation of  $\mathbb{S}$ . However, the transformation destroys the iid property of the sample and a more sophisticated asymptotic analysis is required.

We proceed as follows. For iid bivariate data  $\{(X_i, Y_i), 1 \leq i \leq n\}$  from a distribution in a domain of attraction, define the marginal antiranks by

$$r_i^{(1)} = \sum_{l=1}^n 1_{[X_l \geq X_i]}, \quad r_i^{(2)} = \sum_{l=1}^n 1_{[Y_l \geq Y_i]},$$

that is,  $r_i^{(j)}$  is the number of  $j$ th components that are as large as the  $j$ th component of the  $i$ th observation. Then:

- Transform the data  $\{(X_i, Y_i), 1 \leq i \leq n\}$  using the antirank transform:

$$\{\mathbf{Z}_i; 1 \leq i \leq n\} = \{(k/r_i^{(1)}, k/r_i^{(2)}); 1 \leq i \leq n\}.$$

- Apply the polar coordinate transformation

$$POLAR \left( \frac{k}{r_i^{(1)}}, \frac{k}{r_i^{(2)}} \right) = (N_{i,k}, \Theta_{i,k}).$$

- Estimate  $\mathbb{S}$  with

$$\hat{\mathbb{S}}_{k,n}(\cdot) = \frac{\sum_{i=1}^n \epsilon_{(N_{i,k}, \Theta_{i,k})}((1, \infty] \times \cdot)}{\sum_{i=1}^n \epsilon_{N_{i,k}}((1, \infty])} \Rightarrow \mathbb{S}(\cdot). \quad (4.6)$$

See Resnick [2007], de Haan and Resnick [1993].

The interpretation of Eq. 4.6 is that the empirical probability measure of those  $\Theta$ s whose radius  $N$  is greater than 1 consistently approximates  $\mathbb{S}$ . Hence, we should get a good estimate of  $\mathbb{S}$  by fitting an adequate distribution to the points  $\{\Theta_{i,k}; N_{i,k} > 1\}$ , for a suitable  $k$  (see Section 4.3). Even though we do not know that  $\mathbb{S}$  has a density, often a density estimate is more striking than a distribution function estimate. For example, a mode in the density at  $1/2$  reveals a tendency towards asymptotic dependence, but modes in the density at 0 and 1 exhibit a tendency towards asymptotic independence.

**4.3. Parametric estimation of the spectral density of  $(S, D)$ .** Using the antiranks method described above, we transform the points  $\{(S_i, D_i)\}$  for each decile group separately. Figure 5 shows histograms of the transformed points  $\{\Theta_{i,k}; N_{i,k} > 1\}$ . The histograms suggest that the strength of the dependence between  $S$  and  $D$  decreases as  $R^\vee$  increases, since there is increasing mass towards the ends of the interval  $[0, 1]$  as the  $R^\vee$  goes up. It is certainly apparent that asymptotic independence does not hold in any decile group.

In order to assess the significance of this apparent trend, we review a parametric estimator of the spectral density. The histograms in Fig. 5 show that the spectral density is reasonably symmetric for each decile group, suggesting that the logistic family may be an appropriate parametric model. The logistic family is a symmetric model for the spectral density [Coles, 2001], defined by

$$h(t) = \frac{1}{2} \left( \frac{1}{\psi} - 1 \right) t^{-1-\frac{1}{\psi}} (1-t)^{-1-\frac{1}{\psi}} [t^{-\frac{1}{\psi}} + (1-t)^{-\frac{1}{\psi}}]^{\psi-2}, \quad 0 \leq t \leq 1, \quad (4.7)$$

with a single parameter  $\psi \in (0, 1)$ . For  $\psi < 0.5$ ,  $h$  is unimodal, whereas for increasingly large values of  $\psi > 0.5$ , the density places greater mass towards the ends of the interval  $[0, 1]$ . In fact, asymptotic independence is obtained as  $\psi \rightarrow 1$ , and perfect dependence is obtained as  $\psi \rightarrow 0$ . This allows us to quantify the effect of  $R^\vee$  on the dependence between  $S$  and  $D$ .

We first fit the model in Eq. 4.7 to the data  $\{\Theta_{i,k}; N_{i,k} > 1\}$  within each  $R^\vee$  decile group by maximum likelihood estimation. The log-likelihood function of  $\psi$  based on  $t_1, \dots, t_n$  is

$$\begin{aligned} l(\psi) = & \sum_{i=1}^n \log \left( \frac{1}{\psi} - 1 \right) - \sum_{i=1}^n \left( 1 + \frac{1}{\psi} \right) \log(t_i(1-t_i)) \\ & + \sum_{i=1}^n (\psi - 2) \log(t_i^{-1/\psi} + (1-t_i)^{-1/\psi}), \end{aligned} \quad (4.8)$$

which we maximize numerically for  $0 \leq \psi \leq 1$ . By considering  $\psi$  as a function of  $k$ , we choose a value of  $k$  around which the estimate of  $\psi$  looks stable. Figure 5 shows that the logistic estimates of the spectral

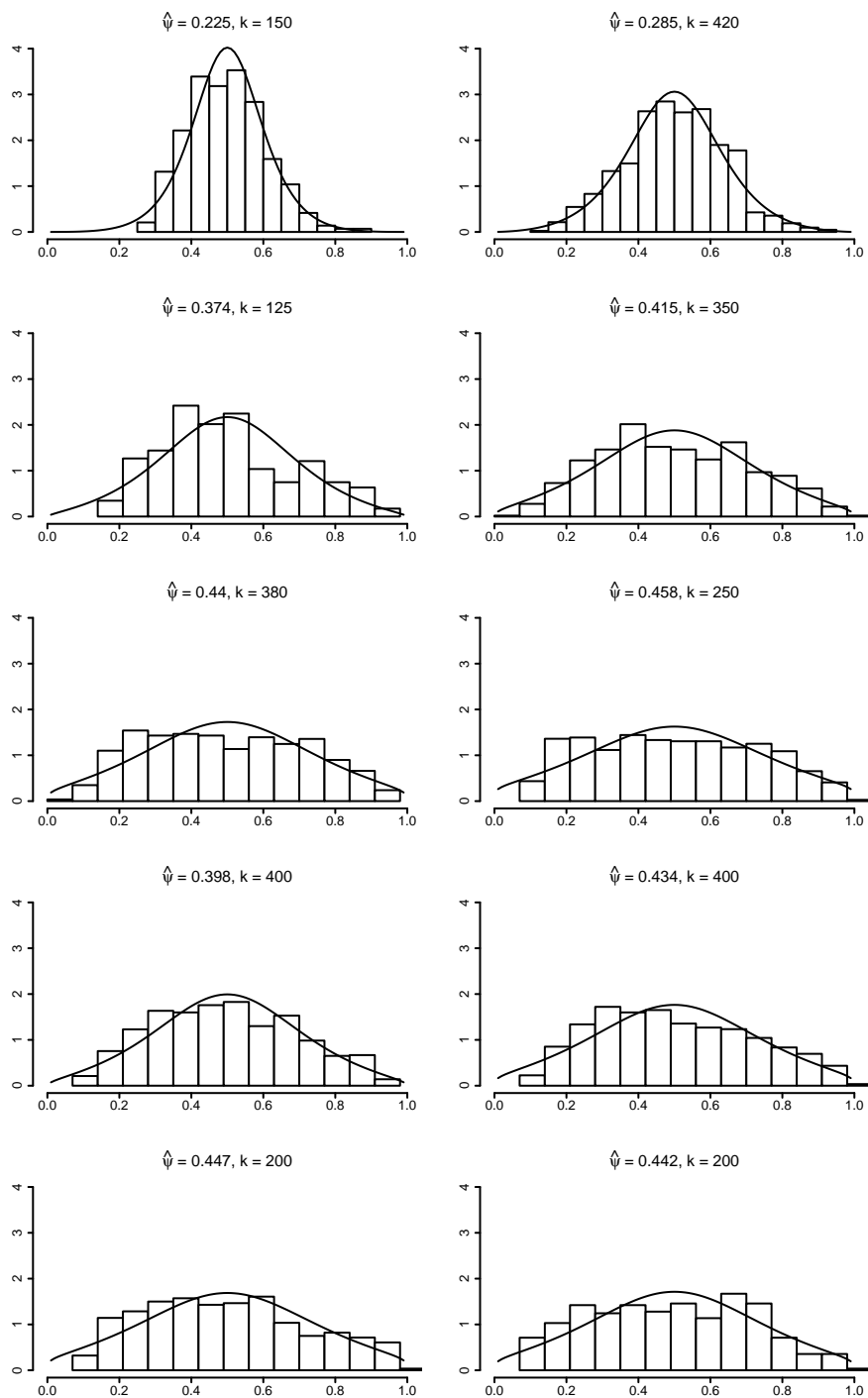


FIGURE 5. Logistic estimates of the spectral density of  $(S, D)$  superimposed on the histograms of the points  $\{\Theta_{i,k}; N_{i,k} > 1\}$ , starting with the 1st decile group from the upper left and going left to right by row



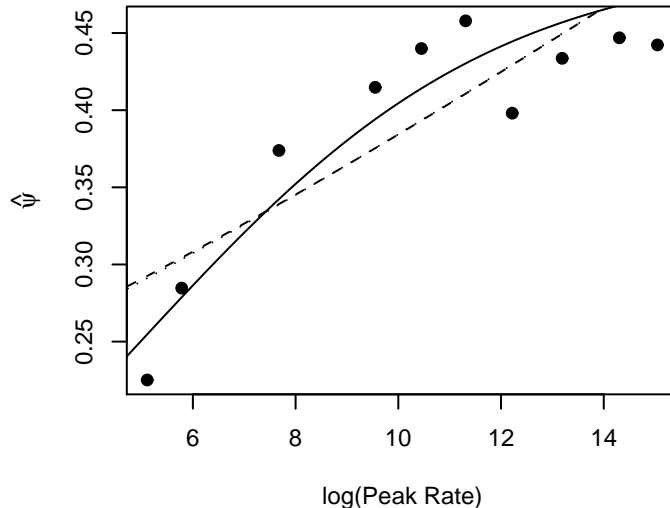


FIGURE 6. Parameter  $\psi$  as a function of  $\log(R^\vee)$  and three linear models of the form given by Eq. 4.9 superimposed: (solid line) link function in Eq. 4.10, (dashed line) logit link, (dotted line) probit link. The logit and probit links are almost indistinguishable in the range of the data

density are in close agreement to the histogram of the points. On top of each plot, we indicate the maximum likelihood estimates of  $\psi$  and the choice of  $k$  in the corresponding decile group. The estimates of  $\psi$  confirm a decline in dependence between  $S$  and  $D$  as the decile group increases, as measured by increasing estimates of  $\psi$ .

We now study the form of this decline by fitting a global trend model simultaneously to all the peak rate decile groups, using the same data (antirank transformed, polar coordinate transformed, thresholded) employed for the separate analyses. In this joint study, the parameter  $\psi$  in Eq. 4.8 is a function of  $R^\vee$  as follows:

$$g^{-1}(\psi) = \beta_0 + \beta_1 \log(R^\vee), \quad (4.9)$$

where  $g$  is a link function. The used of  $\log(R^\vee)$  instead of  $R^\vee$  is a common technique in linear models to improve fit. Since  $\psi \in (0, 1)$ , natural choices of  $g$  are the logit and the probit functions. However, as shown in Fig. 6, the link function

$$g(x) = \frac{0.5}{1 + e^{-x}} \quad (4.10)$$

is more adequate than the usual logit or probit links. The link given by Eq. 4.10 is very similar to the logit link, but confines the possible values of  $\psi$  to the interval  $(0, 0.5)$  and is suggested by the fact that in Fig. 5 the histograms of the points  $\{\Theta_{i,k}; N_{i,k} > 1\}$  put all mass around an apparent mode at 0.5. This behavior corresponds to  $\psi < 0.5$  as previously stated.

Figure 6 exhibits in various ways the logistic parameter  $\psi$  as a function of peak rate using Eq. 4.9. First, we plot the points  $\mathcal{P} = \{(med^{(i)}, \hat{\psi}^{(i)}); 1 \leq i \leq 10\}$ , where  $med^{(i)}$  is the median of the  $\log R^\vee$  variable for sessions in the  $i$ th decile group and  $\hat{\psi}^{(i)}$  is the maximum likelihood estimated logistic parameter in the  $i$ th decile group. In Fig. 6, we superimpose on  $\mathcal{P}$  the estimated Eq. 4.9 using the link function in Eq. 4.10, showing that the goodness of fit of the model in Eq. 4.9 is quite reasonable.

TABLE 2. Summary of estimated linear model given by Eqs. 4.9 and 4.10

	Estimated parameter	Bootstrap standard errors
$\hat{\beta}_0$	-1.432	0.219
$\hat{\beta}_1$	0.288	0.127

To assess the effect of  $R^\vee$  on the dependence structure of  $(S, D)$ , we focus on  $\hat{\beta}_1$ . Observe that Eq. 4.8 gives the log-likelihood of the model for independent observations. Since  $\{\Theta_{i,k}; N_{i,k} > 1\}$  is not an independent sample due to the antirank transform, the classical maximum likelihood theory is not strictly applicable. Hence, to quickly compute the standard error of  $\hat{\beta}_1$  we bootstrap the whole model. However, several authors have shown in the context of heavy-tailed phenomena that if the original sample is of size  $n$ , then the bootstrap sample size  $m$  should be of smaller order for asymptotics to work as desired [Athreya, 1987, Deheuvels et al., 1993, Giné and Zinn, 1989, Hall, 1990, Resnick, 2007]. In connection with the estimation of the spectral measure, the bootstrap procedure works as long as  $m \rightarrow \infty$ ,  $m/n \rightarrow 0$  and  $n \rightarrow \infty$ . Therefore, a bootstrap procedure to estimate the standard error of  $\hat{\beta}_1$  is constructed as follows:

- (i) From the original sample  $\{(S_i, D_i, R_i^\vee); 1 \leq i \leq 44136\}$ , a bootstrap sample  $\{(S_i^*, D_i^*, R_i^{\vee*}); 1 \leq i \leq 10000\}$  is obtained. Notice that the bootstrap sample size is of smaller order than the original sample size. Our choice of  $m = 10000$  owes to the need of having enough data points to perform estimation. However, the choice of the bootstrap sample size is as tricky as choosing the threshold  $k$  used in, say, Hill estimation. Hence, this may be subject of further study.
- (ii) Split the bootstrap sample  $\{(S_i^*, D_i^*, R_i^{\vee*}); 1 \leq i \leq 10000\}$  into 10 groups according to the quantiles of  $R_i^{\vee*}$ .
- (iii) Within each bootstrap decile group, transform the data  $\{(S_i^*, D_i^*); 1 \leq i \leq 1000\}$  using the antirank transform and then transform to polar coordinates to obtain  $\{\Theta_{i,k}^*; N_{i,k}^* > 1\}$ . Here, for each bootstrap decile group we use the same value of  $k$  that is used in the original estimation. These values are shown in Fig. 5.
- (iv) Fit the global linear trend simultaneously to all the bootstrap decile groups, by maximizing Eq. 4.8 with  $\psi$  as a function of  $R^{\vee*}$  as in Eqs. 4.9 and 4.10. Hence, we obtain a bootstrap replication  $\hat{\beta}_{1,b}^*$ .
- (v) Repeat steps (i)-(iv)  $B = 1000$  times and estimate the standard error of  $\hat{\beta}_1$  by the sample standard deviation of the  $B$  replications

$$\widehat{se}(\hat{\beta}_1) = \left\{ \frac{1}{B-1} \sum_{b=1}^B [\hat{\beta}_{1,b}^* - \hat{\beta}_1^*]^2 \right\}^{1/2}, \quad (4.11)$$

where  $\hat{\beta}_1^* = \sum_{b=1}^B \hat{\beta}_{1,b}^* / B$ .

Table 2 summarizes the estimated parameters of the linear model for  $\psi$  and their standard errors. Recall that our model assesses dependence through the value of  $\psi$ . From these results, we conclude that there is a significant effect of the level of  $R^\vee$  in the dependence structure of  $(S, D)$ , since  $\hat{\beta}_1$  is significantly different from 0.

We conclude that Eq. 4.9 jointly with Eq. 4.10 provide an adequate description of the behavior of  $\psi$  across the decile groups.

**4.4. Parametric estimation of the spectral density of  $(R, S)$  and  $(R, D)$ .** We now transform the points  $\{(R_i, S_i)\}$  and the points  $\{(R_i, D_i)\}$  in the 10th decile group using the previously described antirank transform. Figures 7(a) and 7(b) exhibit histograms of the transformed points  $\{\Theta_{i,k}; N_{i,k} > 1\}$  corresponding to the pairs  $(R, S)$  and  $(R, D)$ , respectively. Both histograms look reasonably symmetric, and thus the modeling is done via the logistic family defined by Eq. 4.7.

Figure 7 shows that the fitted logistic models are in close agreement with the empirical distribution of the points  $\{\Theta_{i,k}; N_{i,k} > 1\}$ . Notice that the parameter  $\psi$  of the logistic density corresponding to the pair  $(R, D)$  is closer to 1 than the parameter  $\psi$  of the density corresponding to the pair  $(R, S)$ . This suggests that for

the group of sessions with the highest values of  $R^\vee$ , the scheme  $RD$  (in which  $R$  and  $D$  are independent, at least asymptotically), is more adequate than the scheme  $RS$  (in which  $R$  and  $S$  are independent, at least asymptotically). This conclusion is exactly the opposite to Sarvotham et al. [2005]’s, since they recommend using the scheme  $RS$  for the group with the highest peak rates (that is, their alpha group).

The fact that for the sessions with the highest values of peak rate  $R^\vee$ , we have  $(R, D)$  close to asymptotically independent may have the following interpretation. Users with high bandwidth pay little or no attention to the duration of their downloads; this is expected because such users know that probably their lines are capable of downloading any file, no matter how long it takes.

5. DEPENDENCE STRUCTURE OF  $(S, D, R)$  WHEN  $R$  DOES NOT HAVE HEAVY TAILS

We now investigate the dependence structure of  $(R, S)$  and  $(R, D)$  in the first nine decile groups, that is, those with values of  $R^\vee$  in the decile ranges  $(10(g - 1)\%, 10g\%]$ ,  $g = 1, \dots, 9$ . For these groups, there is evidence that the distribution of  $R$  is not heavy tailed. Moreover, the diagnostics in Section 3.2.1 suggest that  $R \notin \mathcal{D}(G_\gamma)$  for any  $\gamma \in \mathbb{R}$ . However, the other variables  $S$  and  $D$  have heavy tails in these decile groups, and we can make use of the conditional extreme value model [Heffernan and Tawn, 2004, Heffernan and Resnick, 2007, Das and Resnick, 2008a,b] to study the dependence structure of the pairs  $(R, S)$  and  $(R, D)$ .

**5.1. The conditional extreme value model.** Classical bivariate extreme value theory assumes that both variables are in some maximal domain of attraction. When one variable is in a domain of attraction, but the other is not, the conditional extreme value model, or CEV provides a candidate model.

Let  $\mathbf{Z} = (X, Y) \in \mathbb{E} = [0, \infty]^2 \setminus \{(0, 0)\}$  and let  $\mathbb{E}^{(\gamma)}$  be the right closure of  $\mathbb{E}^{(\gamma)} = \{y \in \mathbb{R} : 1 + \gamma y > 0\}$ . The CEV model assumes that  $Y \in \mathcal{D}(G_\gamma)$ ,  $\gamma \in \mathbb{R}$ , with normalizing sequences  $a(t) > 0$  and  $b(t)$  as in Eq. 3.4. In addition, the CEV model assumes that there exist functions  $\alpha(t) > 0$ ,  $\beta(t) \in \mathbb{R}$  and a non-null Radon measure  $\mu$  on the Borel subsets of  $[-\infty, \infty] \times \mathbb{E}^{(\gamma)}$  such that the following conditions hold for any  $y \in \mathbb{E}^{(\gamma)}$ :

(i) For  $\mu$ -continuity points  $(x, y)$ :

$$t\mathbb{P}\left(\frac{X - \beta(t)}{\alpha(t)} \leq x, \frac{Y - b(t)}{a(t)} > y\right) \rightarrow \mu([-\infty, x] \times (y, \infty]), \quad t \rightarrow \infty.$$

(ii)  $\mu([-\infty, x] \times (y, \infty])$  is not a degenerate distribution in  $x$ .

(iii)  $\mu([-\infty, x] \times (y, \infty]) < \infty$ .

(iv)  $H(x) := \mu([-\infty, x] \times (0, \infty])$  is a probability distribution.

The reason for the name CEV is that, assuming  $(x, 0)$  is a  $\mu$ -continuity point:

$$\mathbb{P}\left(\frac{X - \beta(t)}{\alpha(t)} \leq x \mid Y > b(t)\right) \rightarrow H(x), \quad t \rightarrow \infty. \tag{5.1}$$

Therefore, Eq. 5.1 provides a way to study the dependence structure of the components of  $\mathbf{Z}$  when only one is in a maximal domain of attraction.

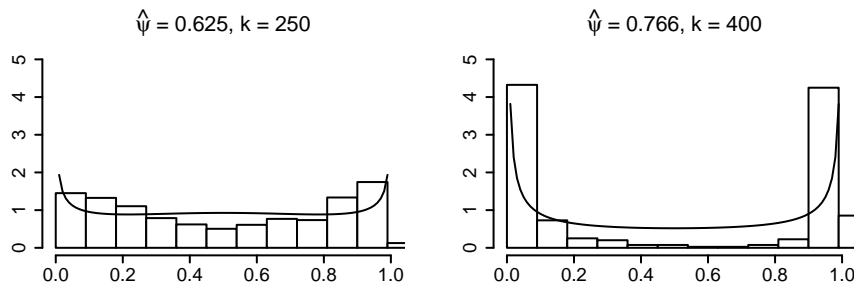


FIGURE 7. Logistic estimates in the 10th decile group superimposed on the histograms of the points  $\{\Theta_{i,k}; N_{i,k} > 1\}$  Left Spectral density of  $(R, S)$  Right Spectral density of  $(R, D)$

**5.2. Checking the CEV model.** We now review a method for checking the adequateness of the CEV model, recently developed by [Das and Resnick \[2008a\]](#). Suppose  $\{(X_i, Y_i); 1 \leq i \leq n\}$  are iid from the CEV model. Define:

- $Y_{(1)} \geq \dots, Y_{(n)}$ : The upper-order statistics of  $Y_1, \dots, Y_n$ .
- $X_i^*, 1 \leq i \leq n$ : The  $X$ -variable corresponding to  $Y_{(i)}$ , also called the *concomitant* of  $Y_{(i)}$ .
- $r_{i,k}^* = \sum_{l=1}^k 1_{[X_l^* \leq X_i^*]}$ : The rank of  $X_i^*$  among  $X_1^*, \dots, X_k^*$ .

The *Hillish statistic* of  $\{(X_i, Y_i); 1 \leq i \leq n\}$  is defined as

$$\text{Hillish}_{k,n} := \frac{1}{k} \sum_{j=1}^k \log \frac{k}{r_{i,k}^*} \log \frac{k}{j}.$$

Under  $H_0 : \{(X_i, Y_i); 1 \leq i \leq n\}$  are iid from a CEV model, [Das and Resnick \[2008b\]](#) proved that as  $k \rightarrow \infty, k/n \rightarrow 0$ , and  $n \rightarrow \infty$ :

$$\text{Hillish}_{k,n} \xrightarrow{P} I_{\mu,H}, \quad (5.2)$$

where  $I_{\mu,H}$  is a constant that depends on  $\mu$  and  $H$  defined in Section 5.1.

Like the Hill estimator, the Hillish statistic depends on the number  $k$ , so we make a *Hillish plot*  $\{(k, \text{Hillish}_{k,n}); k \geq 1\}$  and observe whether the plot has a stable regime. If that is the case, we conclude that the CEV model is adequate for  $(X, Y)$ .

**5.3. Checking the CEV model for  $(R, S)$ .** The CEV model appears as a candidate model for  $(R, S)$  or  $(R, D)$  for any one of the lowest 9 decile groups, since for these groups  $R$  does not appear to be in a domain of attraction, while both  $S$  and  $D$  have heavy tails. We found that the CEV model is adequate for  $(R, S)$  within each of the lowest nine  $R^\vee$ -decile groups. Here we present our results.

Figure 8 shows Hillish plots for checking the CEV model for  $(R, S)$  in the lowest nine decile groups. Apart from the second and third decile groups, all the plots look exceptionally stable. Although the plots do not look as good for the second and third decile groups, we still find a stable regime about the  $k = 800$  upper order statistic, which supports the CEV model for these groups as well. This emphasizes that more detailed structure exists for the beta group of [Sarvotham et al. \[2005\]](#) and that further segmentation reveals more information.

Moreover, observe that the limit constant  $I_{\mu,H}$  varies with the decile group. In effect,  $I_{\mu,H}$  decreases as  $R^\vee$  goes up. Since  $I_{\mu,H}$  depends on the limit  $H$  in Eq. 5.1, this suggests that the conditional distribution of  $R$  given  $S$  varies with the decile group. Hence, the dependence structure of  $(S, D, R)$  depends on the explicit level of  $R^\vee$ .

In addition, the Hillish plots reject the CEV model for the pair  $(R, D)$  in all the decile groups. We have not displayed these plots.

## 6. THE POISSON PROPERTY

There is considerable evidence against the Poisson model as the generating mechanism for network traffic at the packet-level [[Paxson and Floyd, 1995](#), [Willinger et al., 1997](#), [Willinger and Paxson, 1998](#), [Hohn et al., 2003](#)]. However, the classical mechanism of Poisson arrival times, namely human activity generating *many independent* user connections to a server each with *small probability* of occurrence, is still present in the network traffic at higher levels. A significant example is provided by [Park et al. \[2006\]](#), which shows that “navigation bursts” in the server occur according to the Poisson model.

Here we found that, although the Poisson model does not appear to activate the overall network traffic, it does initiate user sessions for any given group of sessions whose peak rate  $R^\vee$  is in a fixed inter-decile range. This allows for quite straightforward simulation within each decile group via a homogeneous Poisson process.

Recall we split the sessions into 10 groups according to the deciles of  $R^\vee$ . For any given decile group, suppose that  $\Gamma_i$  are the starting times of the user sessions in increasing order; if necessary, we relabel sessions within the group. Let  $\Delta_i = \Gamma_{i+1} - \Gamma_i$  be the session interarrival times. A homogeneous Poisson process is

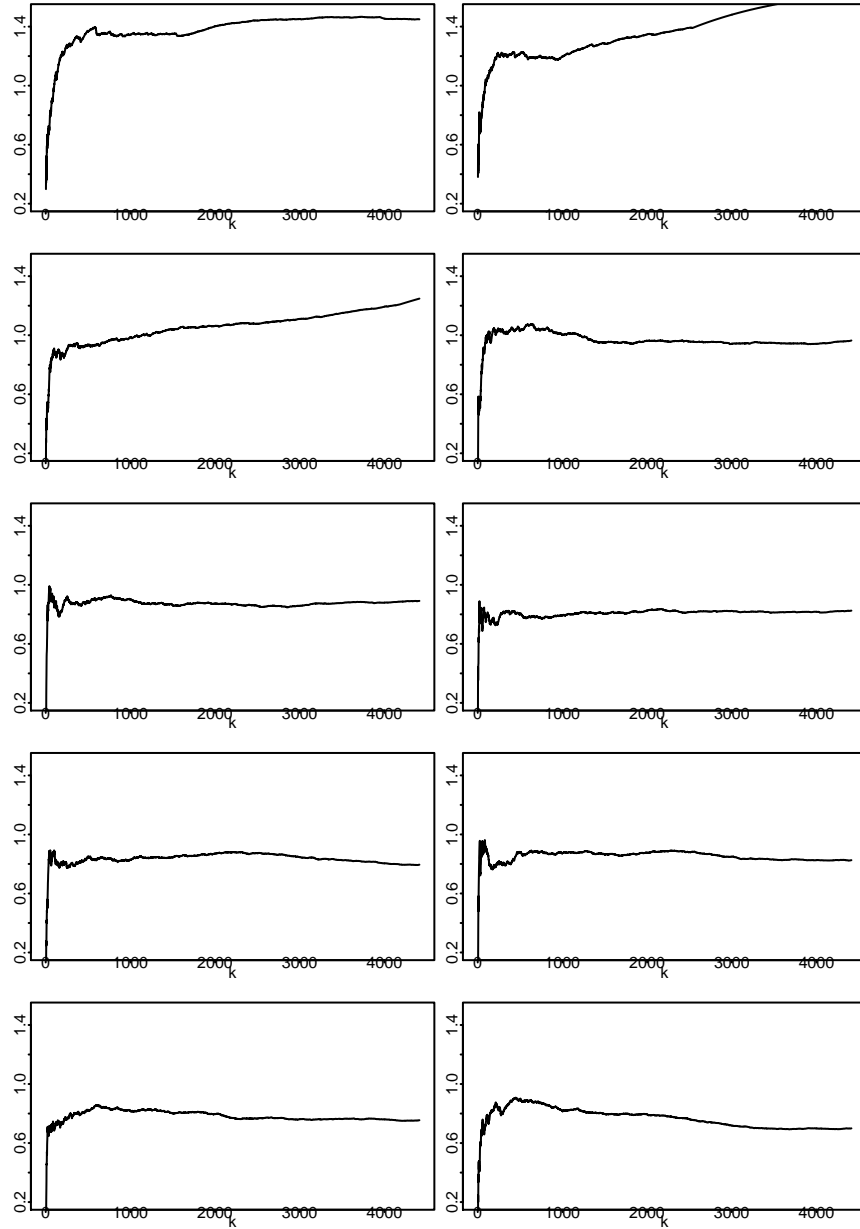


FIGURE 8. Hillish statistic of  $(R, S)$ , starting with the 1st decile group from the upper left and going by row

characterized by  $\{\Delta_i\}$  being iid with the exponential  $\exp(\lambda)$  as the common distribution function, for some parameter  $\lambda > 0$ .

**6.1. Checking the exponential distribution for interarrival times.** We first check that  $\{\Delta_i\}$  may be accurately modeled as exponential random variables within each  $R^V$  decile group. As examples, Fig. 9 *Upper left* and *textitUpper right* panels exhibit exponential QQ plots for  $\{\Delta_i\}$  for the 4th and 10th decile groups, respectively, which compare the quantiles of the empirical and theoretical distributions. It is striking how well a straight line trend is shown, and this result replicates across all the decile groups. However,

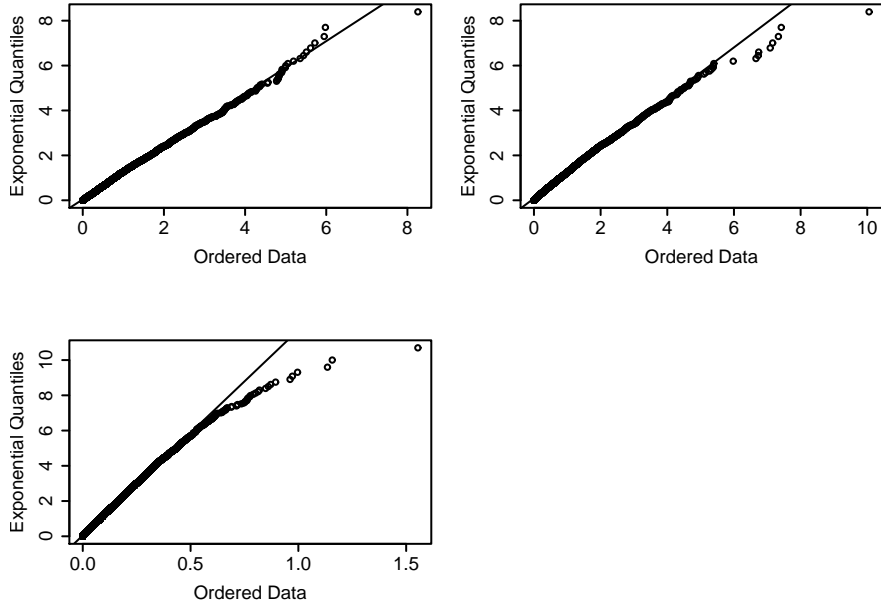


FIGURE 9. Exponential QQ plots of the interarrival times of sessions *Upper left* 4th decile group *Upper right* 10th decile group *Lower left* overall traffic

when all the sessions are put together in a single population, the session interarrival times have right tails noticeably heavier than exponential, as Fig. 9 *Lower left* shows.

Interestingly, we found that the interarrival times within each decile group are not exponentially distributed when rather than using the deciles of  $R^V$  for the segmentation, we use the deciles of any of the two previous predictors of burstiness, namely  $I_\delta$  and  $R_\delta$ .

**6.2. Checking the independence of interarrival times.** Within each decile group, can we use the independence model for  $\{\Delta_i\}$ ? We investigated this question with the sample autocorrelation function. The *sample autocorrelation function (acf)* of  $\Delta_1, \dots, \Delta_n$  at lag  $h$  is defined as

$$\hat{\rho}(h) = \frac{\sum_{i=1}^{n-h} (\Delta_i - \bar{\Delta})(\Delta_{i+h} - \bar{\Delta})}{\sum_{i=1}^n (\Delta_i - \bar{\Delta})^2}.$$

In Section 6.1, we showed  $\{\Delta_i\}$  can be accurately modeled as an exponential random sample, and thus we can safely assume that the variances of  $\Delta_i$  are finite. Therefore, the standard  $L_2$  theory applies and Bartlett's formula from classical time series analysis [Brockwell and Davis, 1991] provides asymptotic normality of  $\hat{\rho}(h)$  under the null hypothesis of independence, namely,

$$\sqrt{n}\hat{\rho}(h) \xrightarrow{d} N(0, 1). \quad (6.1)$$

Based on Eq. 6.1, we can test  $H_0 : \{\Delta_i\}$  are independent by first determining the corresponding (upper) quantile  $z_{1-\alpha}$  of the normal distribution, and then plotting the sample acf as a function of the lag  $h$ . According to Eq. 6.1, approximately  $1 - \alpha$  of the points  $\hat{\rho}(h)$  should lie between the bounds  $\pm z_{1-\alpha} n^{-1/2}$ , and, if so, there is no evidence against  $H_0$ .

Figure 10 *Left* and *Right* panels exhibit sample acf plots for  $\{\Delta_i\}$  for the 4th and 10th decile groups. In each figure, we plot the confidence bounds for an  $\alpha = 0.05$ . We counted 178 and 141 “spikes” coming out of those bounds, respectively. This represent less than 5% of the total of 4414. In general, we found that less



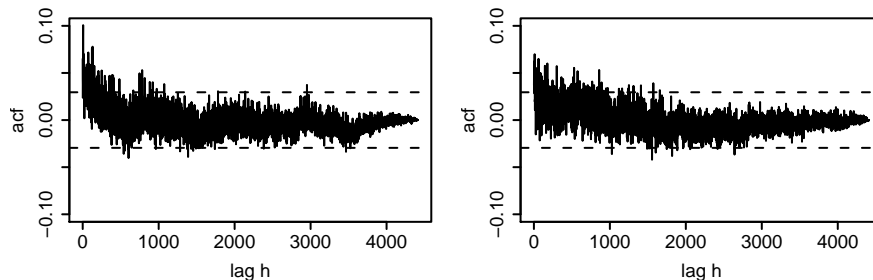


FIGURE 10. Sample autocorrelation functions of  $\Delta_i$  *Left* 4th decile group *Right* 10th decile group

than 5% of the spikes lie outside the bounds for all the decile groups. Based on the sample acf, there is no evidence against the independence of  $\{\Delta_i\}$  within each decile.

## 7. FINAL REMARKS AND CONCLUSIONS

For the purposes of illustration, we have presented our analysis on a data set publicly available as of May 2009 at <http://pma.nlanr.net/Special/index.html> through the National Laboratory for Applied Network Research (NLANR). The particular data file chosen for the analysis is “19991207-125019”, which can be found within a collection of network data traces dubbed *Auckland II* recorded in 1999. We have successfully tested our analyses and proposed models given by Eqs. 4.7 and 4.9 for other data files in the collection *Auckland II*, as well as a more recent collection dubbed *Auckland VIII* recorded in 2003.

Unfortunately, the NLANR website will be shutdown in May 2009. However, the Waikato Internet Traffic Storage or WITS (<http://www.wand.net.nz/wits/>) has expressed a hope to be able to make some of the NLANR’s data sets (in particular, those corresponding to the Auckland’s series) freely available for researchers to download in the near future.

The reason for our choice of the logistic family and the linear trend is because they allow for a simple description of the dependence structure of  $(S, D)$  via the logistic parameter. As depicted in Figs. 5 and 6, the proposed logistic model defined by Eq. 4.7, jointly with the linear trend as in Eq. 4.9, does a sound job of explaining the dependence structure of  $(S, D)$  as a function of the explicit level of the peak rate  $R^\vee$ .

Our findings can yield more accurate simulation methods for network data. The following is an outline of a procedure to simulate network data traces:

- (1) Bootstrap from the empirical distribution of  $R^\vee$  and split the data into, say, 10 groups according to the empirical deciles.
- (2) Conditionally on the decile group, simulate the starting times  $\Gamma$  of the sessions via a homogeneous Poisson process. This means that the Poisson rate depends on the decile group; for example, from the original data set estimate the Poisson rates for each decile group and use them here.
- (3) From  $R^\vee$ , compute  $\psi$  using the estimated linear trend as in Eq. 4.9 and use it to simulate an “angle”  $\Theta$ .
- (4) Simulate the radial component  $N$  as a heavy tailed random variable, for instance the Pareto [Resnick, 2007, de Haan and Resnick, 1993].
- (5) Finally, transform  $(N, \Theta)$  to Cartesian coordinates in order to get  $(S, D)$  and compute  $R = S/D$ .

We are considering details of a software procedure to implement this simulation suggestion.

Our analyses can be readily extended to other segmentation schemes. For instance, heterogeneous traffic comprising different types of applications undoubtedly behaves differently from more homogeneous traffic, a fact used to justify the modeling in D’Auria and Resnick [2008]. Our analyses should provide useful insights by investigating the dependence structure according to the application type.

On another direction, we have shown evidence for the two following models:

- The classical extreme value theory for the pair  $(S, D)$ , in which both components are heavy-tailed.
- The conditional extreme value (CEV) model for the pair  $(R, S)$ , in which only one component, namely  $S$ , is heavy-tailed.

Given the fact that  $R = S/D$ , we are investigating the conditions on the CEV model for  $(R, S)$  that imply the classical model for  $(S, D)$ , and vice versa.

## 8. ACKNOWLEDGEMENT

Early discussions with Janet Heffernan significantly shaped the directions of these investigations and our final effort reflects the benefit of her initial creative inputs. In particular the idea of using link functions in Section 4.4 was hers.

## REFERENCES

- M. Arlitt and C. Williamson. Web server workload characterization: the search for invariants. Master's thesis, University of Saskatchewan, 1996.
- K. B. Athreya. Bootstrap of the mean in the infinite variance case. *Ann. Stat.*, 15(2):724–731, 1987. ISSN 0090-5364.
- A. A. Balkema and L. de Haan. Residual life time at great age. *Ann. Probab.*, 2(5):792–804, 1974.
- J. Beirlant, Y. Goegebeur, J. Teugels, and J. Segers. *Statistics of Extremes*. Wiley Series in Probability and Statistics. John Wiley & Sons Ltd., Chichester, 2004. ISBN 0-471-97647-4. Theory and applications, With contributions from Daniel De Waal and Chris Ferro.
- P.J. Brockwell and R.A. Davis. *Time Series: Theory and Methods*. Springer-Verlag, New York, second edition, 1991.
- S.G. Coles. *An Introduction to Statistical Modeling of Extreme Values*. Springer Series in Statistics. London: Springer. xiv, 210 p. , 2001.
- M. Crovella and A. Bestavros. Self-similarity in world wide web traffic: evidence and possible causes. *IEEE/ACM Trans. Netw.*, 5(6):835–846, 1997.
- S. Csörgő, P. Deheuvels, and D. Mason. Kernel estimates for the tail index of a distribution. *Ann. Stat.*, 13(3):1050–1077, 1985.
- B. Das and S.I. Resnick. Conditioning on an extreme component: Model consistency and regular variation on cones. Technical report, Cornell University, School of ORIE, 2008a. <http://arxiv.org/abs/0805.4373>; submitted to *Bernoulli*.
- B. Das and S.I. Resnick. Detecting a conditional extreme value model. Technical report, Cornell University, School of ORIE, 2008b. <http://arxiv.org/abs/0902.2996>; submitted to *Extremes*.
- B. D'Auria and S.I. Resnick. Data network models of burstiness. *Adv. Appl. Probab.*, 38(2):373–404, 2006.
- B. D'Auria and S.I. Resnick. The influence of dependence on data network models. *Adv. Appl. Probab.*, 40(1):60–94, 2008.
- R.A. Davis and S.I. Resnick. Tail estimates motivated by extreme value theory. *Ann. Stat.*, 12(4):1467–1487, 1984.
- A. C. Davison and R. L. Smith. Models for exceedances over high thresholds. (with discussion). *J. R. Stat. Soc., B*, 52(3):393–442, 1990.
- L. de Haan and A. Ferreira. *Extreme Value Theory: An Introduction*. Springer-Verlag, New York, 2006.
- L. de Haan and L. Peng. Comparison of tail index estimators. *Stat. Neerlandica*, 52(1):60–70, 1998. ISSN 0039-0402.
- L. de Haan and S.I. Resnick. Limit theory for multivariate sample extremes. *Z. Wahrscheinlichkeitstheorie und Verw. Gebiete*, 40(4):317–337, 1977.
- L. de Haan and S.I. Resnick. Estimating the limit distribution of multivariate extremes. *Stoch. Models*, 9(2):275–309, 1993. ISSN 0882-0287.
- L. de Haan and S.I. Resnick. On asymptotic normality of the Hill estimator. *Stoch. Models*, 14(4):849–867, 1998.

- P. Deheuvels, D.M. Mason, and G.R. Shorack. Some results on the influence of extremes on the bootstrap. *Ann. Inst. H. Poincaré Probab. Stat.*, 29(1):83–103, 1993. ISSN 0246-0203.
- A.L.M. Dekkers and L. de Haan. On the estimation of the extreme-value index and large quantile estimation. *Ann. Stat.*, 17(4):1795–1832, 1989.
- D. Dietrich, L. de Haan, and J. Hüsler. Testing extreme value conditions. *Extremes*, 5(1):71–85, 2002.
- H. Drees, Laurens de Haan, and Deyuan Li. Approximations to the tail empirical distribution function with application to testing extreme value conditions. *J. Stat. Plan. Inference*, 136(10):3498–3538, 2006.
- P. Embrechts, C. Kluppelberg, and T. Mikosch. *Modelling Extreme Events for Insurance and Finance*. Springer-Verlag, Berlin, 1997.
- J. Geluk, L. de Haan, S.I. Resnick, and C. Stărică. Second-order regular variation, convolution and the central limit theorem. *Stoch. Process. Appl.*, 69(2):139–159, 1997. ISSN 0304-4149.
- Evarist Giné and Joel Zinn. Necessary conditions for the bootstrap of the mean. *Ann. Stat.*, 17(2):684–691, 1989. ISSN 0090-5364.
- C.A. Guerin, H. Nyberg, O. Perrin, S.I. Resnick, H. Rootzén, and C. Stărică. Empirical testing of the infinite source poisson data traffic model. *Stoch. Models*, 19(2):151–200, 2003.
- P. Hall. On some simple estimates of an exponent of regular variation. *J. R. Stat. Soc., B*, 44(1):37–42, 1982. ISSN 0035-9246.
- P. Hall. Asymptotic properties of the bootstrap for heavy-tailed distributions. *Ann. Probab.*, 18(3):1342–1360, 1990. ISSN 0091-1798.
- J.E. Heffernan and S.I. Resnick. Limit laws for random vectors with an extreme component. *Ann. Appl. Probab.*, 17(2):537–571, 2007. ISSN 1050-5164. doi: 10.1214/105051606000000835.
- J.E. Heffernan and J.A. Tawn. A conditional approach for multivariate extreme values (with discussion). *J. R. Stat. Soc., B*, 66(3):497–546, 2004.
- B.M. Hill. A simple general approach to inference about the tail of a distribution. *Ann. Stat.*, 3(5):1163–1174, 1975.
- N. Hohn, D. Veitch, and P. Abry. Cluster processes: a natural language for network traffic. *IEEE Trans. Signal Process.*, 51(8):2229–2244, 2003. ISSN 1053-587X.
- Xin Huang. *Statistics of Bivariate Extreme Values*. Ph.D. thesis, Tinbergen Institute Research Series 22, Erasmus University Rotterdam, Postbus 1735, 3000DR, Rotterdam, The Netherlands, 1992.
- J. Hüsler and D. Li. On testing extreme value conditions. *Extremes*, 9(1):69–86, 2006.
- S. Keshav. *An Engineering Approach to Computer Networking; ATM Networks, the Internet, and the Telephone network*. Addison-Wesley, Reading, Mass., 1997.
- E.L. Lehmann and J.P. Romano. *Testing Statistical Hypotheses*. Springer Texts in Statistics. Springer, third edition, 2005.
- W.E. Leland, M.S. Taqqu, W. Willinger, and D.V. Wilson. On the self-similar nature of ethernet traffic (extended version). *IEEE/ACM Trans. Netw.*, 2(1):1–15, 1994. ISSN 1063-6692. doi: <http://dx.doi.org/10.1109/90.282603>.
- D. Mason and T. Turova. Weak convergence of the Hill estimator process. In J. Galambos, J. Lechner, and E. Simiu, editors, *Extreme Value Theory and Applications*, pages 419–432. Kluwer Academic Publishers, Dordrecht, Holland, 1994.
- K. Maulik, S.I. Resnick, and H. Rootzén. Asymptotic independence and a network traffic model. *J. Appl. Probab.*, 39(4):671–699, 2002. ISSN 0021-9002.
- A.J. McNeil, R. Frey, and P. Embrechts. *Quantitative Risk Management*. Princeton Series in Finance. Princeton University Press, Princeton, NJ, 2005. ISBN 0-691-12255-5. Concepts, techniques and tools.
- C. Park, H. Shen, J. S. Marron, F. Hernandez-Campos, and D. Veitch. Capturing the elusive poissonity in web traffic. In *MASCOTS '06: Proceedings of the 14th IEEE International Symposium on Modeling, Analysis, and Simulation*, pages 189–196, Washington, DC, USA, 2006. IEEE Computer Society. ISBN 0-7695-2573-3. doi: <http://dx.doi.org/10.1109/MASCOTS.2006.17>.
- V. Paxson and S. Floyd. Wide-area traffic: The failure of poisson modeling. *IEEE/ACM Trans. Netw.*, 3(3):226–244, 1995.

- L. Peng. *Second Order Condition and Extreme Value Theory*. PhD thesis, Tinbergen Institute, Erasmus University, Rotterdam, 1998.
- J. Pickands. Statistical inference using extreme order statistics. *Ann. Stat.*, 3:119–131, 1975.
- R.-D. Reiss and M. Thomas. *Statistical Analysis of Extreme Values*. Birkhäuser Verlag, Basel, third edition, 2007.
- S.I. Resnick. Tail equivalence and its applications. *J. Appl. Probab.*, 8:136–156, 1971.
- S.I. Resnick. *Extreme Values, Regular Variation and Point Processes*. Springer-Verlag, New York, 1987.
- S.I. Resnick. Modeling data networks. In B. Finkenstadt and H. Rootzén, editors, *SemStat: Seminaire Europeen de Statistique, Extreme Values in Finance, Telecommunications, and the Environment*, pages 287–372. Chapman-Hall, London, 2003.
- S.I. Resnick. *Heavy Tail Phenomena: Probabilistic and Statistical Modeling*. Springer Series in Operations Research and Financial Engineering. Springer-Verlag, New York, 2007. ISBN: 0-387-24272-4.
- S.I. Resnick. *Extreme Values, Regular Variation and Point Processes*. Springer, New York, 2008. ISBN 978-0-387-75952-4. Reprint of the 1987 original.
- S. Sarvotham, R. Riedi, and R. Baraniuk. Network and user driven on-off source model for network traffic. *Computer Networks*, 48:335–350, 2005. Special Issue on *Long-range Dependent Traffic*.
- W. Willinger and V. Paxson. Where mathematics meets the Internet. *Not. Am. Math. Soc.*, 45(8):961–970, 1998.
- W. Willinger, M.S. Taqqu, M. Leland, and D. Wilson. Self-similarity in high-speed packet traffic: analysis and modelling of ethernet traffic measurements. *Stat. Sci.*, 10:67–85, 1995.
- W. Willinger, M.S. Taqqu, R. Sherman, and D.V. Wilson. Self-similarity through high variability: Statistical analysis of ethernet lan traffic at the source level. *IEEM/ACM Trans. on Netw.*, 5(1):71–86, 1997.
- W. Willinger, V. Paxson, and M.S. Taqqu. Self-similarity and heavy tails: Structural modeling of network traffic. In R.J. Adler, R.E. Feldman, and M.S. Taqqu, editors, *A Practical Guide to Heavy Tails. Statistical Techniques and Applications*, pages 27–53. Birkhäuser Boston Inc., Boston, MA, 1998.
- Y. Zhang, L. Breslau, V. Paxson, and S. Shenker. On the characteristics and origins of internet flow rates. ACM Sigcom 2002 Conference, Pittsburgh, Pa; August 19-23, 2002.

LUIS LÓPEZ-OLIVEROS, DEPARTMENT OF STATISTICAL SCIENCE, CORNELL UNIVERSITY, ITHACA, NY 14853  
*E-mail address:* 11278@cornell.edu

PROF. SIDNEY RESNICK, SCHOOL OF OPERATIONS RESEARCH AND INFORMATION ENGINEERING, CORNELL UNIVERSITY, ITHACA, NY 14853  
*E-mail address:* sir1@cornell.edu